MECHANICAL CHARACTERIZATION OF FOAM-CEMENT INTERFACE UNDER SELECTED LOADING CONDITIONS

Gianluca Tozzi[1], Qing-Hang Zhang[1], Colin Lupton[1], Jie Tong[1],

Teodolito Guillen[2], Arne Ohrndorf[2], Hans-Jurgen Christ[2]

[1]Mechanical Behaviour of Materials Laboratory
School of Engineering, University of Portsmouth, UK
[2]Institut für Werkstofftechnik
University of Siegen, Germany

For correspondence:

Prof. Jie Tong, Ph.D.
Mechanical Behaviour of Materials Laboratory
School of Engineering
University of Portsmouth
Anglesea Road
Portsmouth PO1 3DJ
UK
Tel: 0044-9284-2326
Fax: 0044-9284-2351
Email: jie.tong@port.ac.uk

ABSTRACT

Open-cell AlSi7Mg (45ppi) foam was employed as trabecular bone substitute and used to interdigitate with acrylic bone cement to form foam-cement interface samples. The interfacial mechanical performance of such bone-cement models was investigated under tension, mixed-mode, shear and step-wise compression loading conditions using experimental protocols reported in Wang et al. [1] and Tozzi et al. [2]. For the step-wise compression, Image-Guided Failure Assessment (IGFA) of the foam-cement interface was carried out to monitor the microdamage evolution with load. Finite element (FE) models were also built from μCT images of the samples in order to predict the foam-cement behaviour and interfacial damage. The results show that the foam-cement mechanical responses under tension (0°), shear (90°) and mixed-mode (22.5°; 45°; 67.5°) loading conditions are broadly similar to those obtained from bone-cement interface samples under the same loading conditions, with the exception of compression where the response from the foam-cement interface is much lower than that of bone-cement interface.

Keywords: Open-cell foams, bone-cement interface, foam-cement interface, mixed-mode loading, step-wise compression, μCT, finite element analysis

1 Introduction

It is widely accepted that the lasting integrity of the bone-cement interface is essential to the success and longevity of cemented hip replacements [3, 4]. A number of studies have been carried out on bone-cement interface under tensile [1, 5], shear [1, 6] and mixed-mode [1, 7] loading conditions. Recently, novel experimental techniques, such as Digital Image Correlation (DIC) and Image-Guided Failure Assessment (IGFA), have been employed to investigate the micromechanical behaviour and the local deformation and microdamage evolution of bone-cement interface in tension [8], tension-compression [9], shear fatigue [10], multi-axial [11] and step-wise compression [2] loading conditions.

Most of the works cited are based on human cadaver or bovine bones to interface with cement. Although these are close to clinical conditions and are often preferred choices, the repeatability of the experiments is generally poor due to the large variation in the mechanical properties of cancellous bone dependent of anatomic site and age [12-16]. For this reason it is desirable to employ analogous bone models with prescribed morphological and mechanical properties to mimic biological tissues, in order to remove some of the inherent uncertainties for biomechanical research purposes.

Synthetic bone analogue materials are often used as a substrate for testing and evaluation of cementing techniques. Open-cell reticulated carbon foams were used as trabecular bone analogous to examine the difference in cement penetration and distribution with different viscosities for resurfacing arthroplasty [17]. More recently, the same foam materials were also used to obtain real-time measurements of cement pressure and temperature related to a range of cementing techniques and conditions [18]. Open-cell rigid polyurethane foam was used by Zhao et al. [19] to simulate the bone-cement micromechanics at trabecular level in order to develop a novel methodology that could be used for specimen-specific FE models of bone–cement composites, allowing the mechanical behaviour at the interface to be examined in more detail.

In our previous work, mechanical testing and morphological analysis using μCT and finite element (FE) modelling were carried out to characterise three selected open-cell metallic foams (AlSi7Mg (30ppi & 45ppi); CuSn12Ni2 (30ppi)), and their apparent mechanical properties, morphology and local damage progression were compared with those obtained from bovine trabecular bone [20]. A step forward in the characterisation of such open-cell foams for cemented arthroplasty simulation is to examine the mechanical performance of the foam-cement system under complex loading conditions relevant to physiological load cases, so that a more comprehensive mechanical characterisation of the foam-cement interface may be developed towards using such analogous materials as bone substitutes for biomechanical studies.

In the current study an open-cell AlSi7Mg (45ppi) foam was selected as an analogous model for its resemblance to bovine trabecular bones [20] in morphology. Foam-cement coupons were produced, similarly to the bovine trabecular bone-cement samples studied before [1]. The foam-cement composites were mechanically tested under tensile, shear, mixed-mode and step-wise compression loading conditions, using the experimental protocols for bone-cement interface characterisation [1, 2]. FE simulations were performed on a typical foam-cement model under compression, tension and shear loading conditions. The predicted apparent behaviour and the simulated local interfacial damage were compared with the correspondent values obtained from the bone-cement specimens.

2 Methods

2.1 Specimens

The open-cell AlSi7Mg (45ppi) foam material (m-pore GmbH) was used for this study, which has a volume fraction (FV/TV) of 0.16±0.008 [20]. Foam strips were used to interdigitate with acrylic bone cement (Simplex P, Stryker, UK) to create foam-cement interface coupons, following the same procedure reported by Wang et al. [1] for bone-cement preparation. Rectangular foam-cement samples were machined to the same size of the bone-cement [1, 2], as shown in Fig.1a, using a low speed diamond saw with constant mineral oil irrigation to avoid abnormal high temperature with a potential for local melting of the metal.

2.2 Tensile, shear and mixed-mode testing

The loading device used in Wang et al. (2010) for bone-cement interface testing was adopted to allow tensile (θ=0°), shear (θ=90°) and selected mixed-mode (θ=22.5°; 45°; 67.5°) loads to be applied (Fig.1b) on the foam-cement composites. A servo-hydraulic testing machine (MTS 810) was used for the experiments and all the tests were conducted in air at room temperature. The foam-cement specimens were fixed in custom grips at prescribed loading angles and loaded to complete failure under displacement control at a rate of 0.01 mm/s. The relative opening displacements were read directly from the LVDT of the machine, while the sliding displacements were measured by means of an extensometer (Sandler EXA 15-5). The vector sums of the total displacements were calculated and used to plot against the loads, recorded by a 2 kN load-cell (ME System). A total of 10 samples were tested at the 5 selected loading angles (0°, 22.5°; 45°; 67.5° and 90°).

2.2 Step-wise compression testing

Step-wise compression testing of the samples (n=5) was performed using a micromechanical loading stage (Deben Ltd, UK) in combination with time-lapsed μCT imaging (Fig.1c). The samples were first glued onto the lower compressive platen, whilst a small preload was applied through the top platen connected to the actuator to ensure a good end contact. Full details of the experimental apparatus and procedures were reported in Tozzi et al. [2].

The specimens underwent μCT analysis (CT X-Ray Inspection System, X-Tek Systems Ltd) prior to testing and a complete data acquisition was performed (V=60 kV, I=140 μA, voxel size=20 μm, rotational step=0.19°/360°, acquisition time=90 min). The 3D reconstruction of the samples was obtained using VG StudioMax 2.0 software (Volume Grapics, GmbH).

The specimens were step-wise compressed at the two selected displacements [2] corresponding approximately to the ultimate apparent strength and just before the final failure, respectively. At each displacement step a relaxation time of about 15 mins was allowed before CT imaging and data acquisition procedure were carried out. All tests were conducted under displacement control at a constant cross head speed of 0.01 mm/s.

2.2 Finite Element Modelling

CT images of the region of interest of a typical foam-cement specimen were imported into Avizo 6.3 (Visualization Sciences Group, Mérignac, France) for FE model generation, in which the foam and cement

structures were modelled individually based on the threshold values. Before meshing, the cement volume was shrunk by one voxel (20 μm) to ensure a good apposition of the two constituents. The generated foam-cement composite model consists of 1,740,135 four-node tetrahedral elements and 379,637 nodes (Fig. 2a). The detailed process of three-dimensional reconstruction and FE mesh generation of the foam-cement interface model followed a protocol reported elsewhere [21]. The bone-cement interface model (BC01) used in Zhang et al. [21] is shown here for comparison (Fig.2b).

The AlSi7Mg alloy and cement were both assumed as isotropic bi-linear elastic-plastic material. The elastic modulus, Poisson's ratio and yield stress of cement were assumed as 3 GPa, 0.33 and 40 MPa, respectively [22], while the corresponding values for AlSi7Mg alloy were assumed to be 70 GPa, 0.3 and 150 MPa, respectively [20]. The interaction between the surface of the foam and that of the cement was modelled as surface-to-surface finite sliding contact, with a friction coefficient of 0.4.

All the simulations of the foam-cement interface model were performed on the FE solver ABAQUS 6.10 (Dassault Systèmes, RI, USA), using large deformation to account for geometrical nonlinearity. The loading and boundary conditions were applied to the model in an attempt to mimic those in the experiments. For the simulation of compression and tension, the bottom surface of the cement was fully constrained in all degrees of freedom while a uniaxial displacement, in compression and tension, respectively, was applied incrementally to the top surface of foam up to 0.3 mm. To mimic the shear test condition, two additional rigid plates were tied to the two opposite sides of the foam-cement model, as shown in Fig. 2a. The rigid plates were positioned such that the bottom edge of the upper plate and the top edge of the lower plate were contained in the same transverse plane of the model. The lower plate was fully constrained while a horizontal displacement of 0.3 mm was applied to the upper plate to generate shear loading. The same conditions were also applied to the bone-cement model (Fig. 2b). The predicted apparent stress-displacement curves of the models were then compared against the obtained experimental results. In addition, the predicted von Mises stress distributions of the two interface models were compared also.

3 Results

The mean apparent interfacial strength for the foam-cement interface compares well with that of the bone-cement interface reported by Wang et al. [1] under the tension (0°), shear (90°) and mixed-mode (22.5°; 45°; 67.5°) loading conditions (Fig. 3). Specifically the foam-cement behaviour seems to be similar to that of bone-cement responses under tension and mixed-mode, with the mechanical response increasing with the increase of the loading angle and reaching the maximum under shear loading in both cases. The average apparent strength for the foam-cement samples ranges from 0.53 MPa in tension to 5.34 MPa in shear, compared with 1.48±0.85 MPa and 4.09±3.66 MPa for the bone-cement interface under tensile and shear loading conditions, respectively [1].

The FE predicted apparent stress-displacement responses of the foam-cement and bone-cement models are compared with those obtained experimentally for tension (Fig. 4a) and shear (Fig. 4b) loading conditions. The models seem to have captured the essence of the experimental responses, although not all the details. At a displacement of 0.3 mm, the calculated interfacial shear stresses of the foam-cement and bone-cement models were 3.8 and 3.0 times higher than their corresponding values under tension, respectively (Fig. 4). Whilst the FE

for the bone-cement case appeared to be in a broad agreement with the experimental data, the foam-cement predictions (Fig. 4a & b) resulted in an overestimation of the mean experimental stiffness for tensile and in particular for shear.

Fig. 5 (I & II) presents some of the progressive microdamage during the step-wise compression in representative 3D sub-volumes for both foam-cement and bone-cement composites. The IGFA analysis for all the foam-cement interface samples (n=5) showed similar patterns where the predominant deformation was found to initiate in the foam region, whilst the cement region appeared to be unaffected even at the final failure stage, as shown in Fig. 5(I). Also, for the foam-cement case, virtually no load transfer occurred at the interface, as opposed to the bone-cement case (Fig. 5(II) [2]). In the latter case the main load transfer occurred in the first contact region of the bone-cement interface, resulting in progressive microdamage including bending and buckling of trabeculae adjacent to the interdigitated region. In the foam-cement samples, strut bending and buckling were observed in the foam body rather than near or at the foam-cement interface (Fig. 5(I)).

The stress-displacement responses of the five foam-cement samples tested under compression are shown in Fig. 6a, together with the FE simulated response. Due to viscoelasticity some stress relaxation occurred during the hold period while the imaging was carried out, resulting in discontinuities in the stress-displacement curves. The ultimate apparent compressive strength for the five samples was estimated as 0.90±0.05 MPa. The predicted stress-displacement behaviour compares reasonably well in terms of simulated stiffness with the experimental data, with the prediction slightly overestimating the experimental corridor formed by the responses from the five specimens. For comparison the bone-cement interfaces tested under the same loading conditions are shown in Fig. 6b, and the ultimate apparent compressive strength for the five samples was estimated as 4.93±1.10 MPa [2], differing considerably from that of foam-cement response. Although FE predictions capture the elastic modulus reasonably well, the prediction overestimated the ultimate compressive strength for foam-cement samples, whilst underestimated the ultimate compressive strength for bone-cement samples.

Fig.7 shows the von Mises stress distribution in the foam/bone and cement of the two types of specimen models under (a) compression, (b) tension and (c) shear when a displacement of 0.3 mm was applied to the models. Similarly to the bone-cement case, the foam region sustained most of the load under tension and compression, with the foam body sustaining almost the entire load outside the interdigitated region, as opposed to shared between the bone and the bone-cement interdigitated region. For the foam-cement model, only the top contact surface with the cement carried some loads, with localised stress concentrations confined to the contact surface and little evidence of load transfer to the cement. As a result, the foam-cement interface seemed to be far less efficient than bone-cement interface in load transfer under tension and compression. Under shear loading condition, the two models showed similar stress distribution patterns where the highly stressed elements appear to be more influenced by the loading mode than by the material characteristics.

4 Discussion

In the current study, the apparent mechanical behaviour and local micro-damage of an AlSi7Mg foam-cement interface were examined under selected loading conditions to explore the performance of such open-cell foam materials as potential substitutes for trabecular bone in cement fixation studies. Under tension and shear, the experimental stress-displacement curves (Fig. 4) exhibit similar characteristics, with an initial linear

behaviour followed by non-linear hardening to reach peak load, then by substantial strain softening until complete debonding of the interface. Although only two foam-cement samples were tested for each loading condition, no significant variation is found in the results, with the only exception for the shear case (90°) as shown in Fig. 4b. This is consistent with that reported in Wang et al. [1] for the bone-cement interface, where the highest interfacial strength and scatter (4.09±3.66 MPa) is also found in shear, as opposed to the mixed mode and tension (1.48±0.85 MPa). Although the interfacial strength in foam-cement samples appear to be lower than that of bone-cement interface under tension, the behaviour appears to be similar in shear for both cases. The apparent tensile strength obtained in the present study (0.53 MPa) is in the lower range for lab-prepared bovine [1] and also human cadaveric bone-cement interface (1.28±0.79 MPa) reported by Mann et al. [5]. For shear the present result of 5.34 MPa is well within the experimental corridor obtained by Wang et al. [1] but higher than the cadaveric result 2.25±1.49 MPa [6], although a range of shear strength such as 4-11 MPa from Dohmae et al. [23], 5-7 MPa from Bugbee et al. [24] and 6-15 MPa from Bean et al. [25] have been reported in literature. Under the mixed mode loading conditions, the foam-cement showed the same increase in strength with the loading angle (r^2=0.68), as observed in Wang et al. [1] for the bone-cement interface (r^2=0.77); and the results are in a broad agreement with those of Mann et al. [6]. When shear is the predominant component an increase in the interfacial strength for both foam and bone cement interfaces was observed, suggesting that shear action may not be very sensitive to foam/bone material properties. Similar findings were reported for other two open-cell metallic foams (30ppi AlSi7Mg & 30ppi CuSn12Ni2) used as bone analogous models for cemented biomechanical testing [26]. It needs to be pointed out that the apparent model behaviour under shear may be greatly affected by the location to which the shear load is applied. The results from the FE analysis show that the apparent shear strength can vary significantly if the shear displacements are applied differently. In Zhang et al. [21], the shear displacement was applied to the top surface of the bone and the resulting shear strength was lower than that under tensile loading. Nevertheless the mechanical responses from the foam-cement interface and the bone-cement interface are in the same order and by large do not deviate significantly.

Under compression, however, the interfacial strength of the foam-cement interface is found much lower than that of bone-cement interface (< 1 MPa for foam-cement vs 3.5 – 6 MPa for bone-cement, Fig. 6b). This may be attributed to the higher contribution of the foam material on the overall response of the interface, where the microstructural deformation within the foam body largely defined the mechanical response of the interface sample under compression. Three dimensional volume visualisation of damage evolution in the foam-cement interface during step-wise compression shows that the foam region sustained almost the deformation, and the main damage resulted in progressive damage of struts mainly due to bending and buckling (Fig. 5(I)). There is virtually no load transferred to the cement mantle (Fig. 7a). The apparent behaviour of such composite structures is dictated by both the low volume fraction cellular solids (0.16±0.008 for 45ppi AlSi7Mg & 0.25±0.07 for trabecular bovine bone [20]) and the low strength of the foam as the mechanical responses of the foam-cement samples are very close to those of the foam solid itself under the same loading condition. This is in contrast to the damage mechanism for trabecular bone-cement interface [2], where a more effective load transfer to the bone-cement interdigitated regime (Fig. 5(II)) was observed. Due to the low volume fraction and predominantly rod-like open-cell structure, there is nearly no partially interdigitated area in the foam-cement

model, as opposed to the trabecular bone-cement model. The cement stress in the foam-cement interface is therefore only concentrated at the top contact surface, while the load was transferred across the bone-cement interface through a larger volume/area. This is consistent with our previous study on bone-cement interface [21], in that the interfacial features are more important than the material characteristics in dictating the interfacial mechanical behaviour.

With exception of compression, the use of metallic foam materials to interface with cement appears to have produced similar interfacial responses under tension, and shear loading conditions, as shown in Fig. 4, although load transfer seems largely ineffective in the cases of foam-cement interface (Fig. 7). The main deformation occurred in the foam part in the foam-cement samples, as opposed to mainly in the interdigitated region in bone-cement samples.

Although the simulated interfacial responses under different loading conditions agreed reasonably with the experimental results, the FE model predicted higher initial stiffness of the foam-cement specimen than the correspondent experimental values (Fig. 4, 6a). For compression, this difference might be attributed to the end and side artefacts of the experimental model [27, 28], as well as local micro-defects in the material and/or micro-damage introduced during sample preparation. Thus the predicted compressive behaviour of the foam-cement FE model is only slightly higher than the experimental results (Fig. 6a). These results are in a broad agreement with the findings reported by Guillen et al. [20] where cylinders made of the same foam (AlSi7Mg, 45ppi) were tested under compression. In the latter a greater mechanical response was also predicted by the micro-FE model, although this was not supported by the apparent mechanical properties measured. Under tension and shear, however, the main reason for the differences may be the difficulties in mimicking the actual loading and boundary conditions as those in the experiments. As discussed above, the chosen planes to which the load was applied in shear can significantly alter the predicted strength. Under tension, the localised deformation near the grips cannot be correctly mimicked by the FE model, which might affect the predicted tensile stress-displacement response. Under tension and compression the simulated results are similar whilst the experimental results differ significantly, suggesting that the FE method was unable to discriminate the effect of loading mode.

Admittedly the results obtained from this study are based on the analysis of a limited number of samples using only one open-cell foam material. Nevertheless the results may be of interest in exploring analogous materials for biomechanical studies of cement fixation behaviour amongst others.

5 Conclusions

Interfacial behaviour of metallic foam-cement interface specimens has been studied under tension, mixed mode (including shear) and compression loading conditions using both experimental and finite element analysis, and the results were compared with those obtained using bovine trabecular bone-cement interface. The foam-cement mechanical performance under tension (0°), shear (90°) and mixed-mode (22.5°; 45°; 67.5°) loading conditions was found to be compatible with those obtained from the bone-cement specimens under the same conditions; whilst under compression, the foam-cement interfacial strength was found to be much lower than the corresponding bone-cement cases. Image-guided failure analysis showed virtually no load transfer in the foam-cement samples, unlike the bone-cement samples where the load transfer occurred mainly in the interdigitated contact region.

Despite these differences, a similar pattern of microdamage evolution due to struts/trabeculae bending and buckling was observed. Although it remains a challenge to find an analogous material that mimics both the apparent mechanical properties of trabecular bone and its microarchitecture, the current study might be a step towards this direction.

Conflict of interest statement

None.

Acknowledgements

The authors gratefully acknowledge Stryker UK for donating the bone cement. Numerical computations were performed on the Sciama High Performance Compute (HPC) cluster which is supported by the ICG, SEPNet and the University of Portsmouth.

REFERENCES

[1] Wang JY, Tozzi G, Chen J, Contal F, Lupton C, Tong, J. Bone–cement interfacial behaviour under mixed mode loading conditions. J. Mech. Behav. Biomed. Mater. 2010; 3:392–398.

[2] Tozzi G, Zhang Q-H, Tong J. 3D real-time micromechanical compressive behaviour of bone-cement interface: experimental and finite element studies. J. Biomech. 2012; 45:356-363.

[3] Stocks GW, Freeman MA, Evans SJ. Acetabular cup migration: prediction of aseptic loosening. J. Bone Joint Surg. Br. 1995; 77:853-861.

[4] Thanner J, Karrholm J, Malchau H, Herberts P. Poor outcome of the PCA and Harris-Galante hip prostheses. Randomized study of 171 arthroplasties with 9-year follow-up. Acta Orthop. Scand. 1999; 70:155-162.

[5] Mann KA, Ayers DC, Werner FW, Nicoletta RJ, Fortino MD. Tensile strength of the cement-bone interface depends on the amount of bone interdigitated with PMMA cement. J. Biomech. 1997; 30:339-346.

[6] Mann, K.A., Werner, F.W., Ayers, D.C., 1999. Mechanical strength of the cement-bone interface is greater in shear than in tension. J. Biomech. 32, 1251-1254.

[7] Mann KA, Mocarski R, Damron LA, Allen MJ, Ayers DC. Mixed-mode failure response of the cement-bone interface. J. Orthop. Res. 2001; 19:1153-1161.

[8] Mann, K.A., Miller, M.A., Clearly, R., Janssen, D., Verdonschot, N., 2008. Experimental micromechanics of the cement-bone interface. J. Orthop. Res. 26(6), 872-79.

[9] Miller MA, Eberhardt AW, Clearly R, Verdonschot N, Mann KA. Micromechanics of postmortem-retrieved cement-bone interfaces. J. Orthop. Res. 2010; 28(2):170-7.

[10] Mann KA, Miller MA, Race A, Verdonschot N. Shear fatigue micromechanics of the cement-bone interface: an in vitro study using digital image correlation techniques. J. Orthop. Res. 2009; 27(3):340-6.

[11] Miller MA, Race A, Waanders D, Clearly R, Janssen D, Verdonschot N, Mann KA. Multi-axial loading micromechanics of the cement-bone interface in post-mortem retrievals and lab-prepared specimens. J. Mech. Behav. Biomed. Mater. 2011; 4:366-74.

[12] Goldstein SA. The mechanical properties of trabecular bone: dependence on anatomic location and function. J. Biomech. 1987; 20:1055–61.

[13] Keaveny TM, Hayes WC. A 20-year perspective on the mechanical properties of trabecular bone. J. Biomech. Eng. 1993; 15:534–42.

[14] Keaveny TM, Morgan EF, Niebur GL, Yeh OC. Biomechanics of trabecular bone. Annu Rev Biomed Eng. 2001; 3:307-333.

[15] Linde F. Elastic and viscoelastic properties of trabecular bone by a compression testing approach. Dan. Med. Bull. 1994; 41:119–38.

[16] Gibson LJ. Biomechanics of cellular solids. J Biomech. 2005; 38(3):377-399.

[17] Bitsch RG, Heisel C, Silva M, Schmalzried TP. Femoral cementing technique for hip resurfacing arthroplasty. J. Orthop. Res. 2007; 25(4):423-31.

[18] Bitsch RG, Loidolt T, Heisel C, Schmalzried TP. Cementing techniques for hip resurfacing arthroplasty: in vitro study of pressure and temperature. Femoral cementing technique for hip resurfacing arthroplasty. J. Arthroplasty 2011; 26(1):144-51.

[19] Zhao Y, Robson Brown KA, Jin ZM, Wilcox RK. Trabecular level analysis of bone cement augmentation: a comparative experimental and finite element study. Ann. Biomed. Eng. 2012; 40(10):2168-76.

[20] Guillen T, Zhang Q-H, Tozzi G, Ohrndorf A, Christ H-J, Tong J. Compressive behaviour of bovine cancellous bone and bone analogous materials, microCT characterization and FE prediction. J. Mech. Behav. Biomed. Mater. 2011; 4:1452-61.

[21] Zhang Q-H, Tozzi G, Tong J. Micromechanical damage of trabecular bone-cement interface under selected loading conditions: a finite element study. Computer Methods in Biomechanics and Biomedical Engineering 2012; in press.

[22] Lewis G. Properties of acrylic bone cement: State of the art review. Journal of Biomedical Materials Research. 1997; 38(2):155-182.

[23] Dohmae Y, Bechtold JE, Sherman RE, Puno RM, Gustilo RB. Reduction in cement-bone interface shear strength between primary and revision arthroplasty. Clin. Orthop. Rel. Res. 1988; 236:214-220.

[24] Bugbee WD, Barrera DL, Lee AC, Convery FR. Variations in shear strenght of the bone-cement interface in the proximal femur. Trans. Orthop. Res. 1992;17:22.

[25] Bean DJ, Hollis JM, Woo SL, Convery FR. Sustained pressurization of polymethylmethacrylate: a comparison of low- and moderate-viscosity bone cements. J. Orthop. Res. 1988; 6:580-584.

[26] Tozzi G. In vitro studies of bone-cement interface and related work on cemented acetabular replacement. University of Portsmouth (UK) 2012; PhD Thesis.

[27] Keaveny TM, Pinilla TP, Crawford RP, Kopperdahl DL, Lou A. Systematic and random errors in compression testing of trabecular bone. J. Orthop. Res. 1997; 15(1):101-10.

[28] Un K, Bevill G, Keaveny TM. The effects of side-artifacts on the elastic modulus of trabecular bone. J Biomech. 2006; 39(11):1955-63.

FIGURES & CAPTIONS

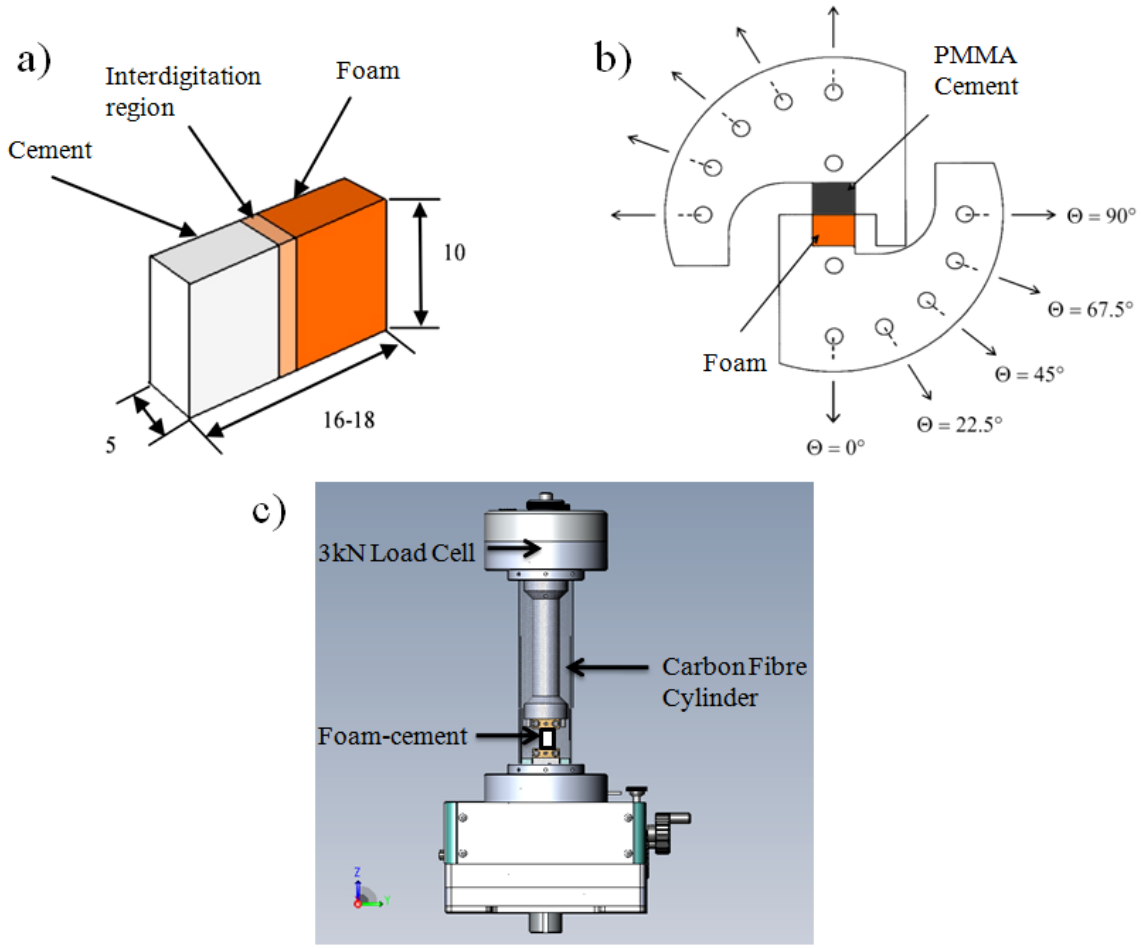

Fig.1 (a) The foam-cement interface sample used in this study (all dimensions are in mm); (b) a schematic of the loading arrangement for tensile (0°), shear (90°) and mixed mode (22.5°, 45°, 67.5°) loading conditions; (c) the micromechanical loading stage (LS) used to apply the load in stepped compression. Bone-cement interface coupons with the same dimensions, tested under the same loading conditions (b-c), are used for comparison [1, 2].

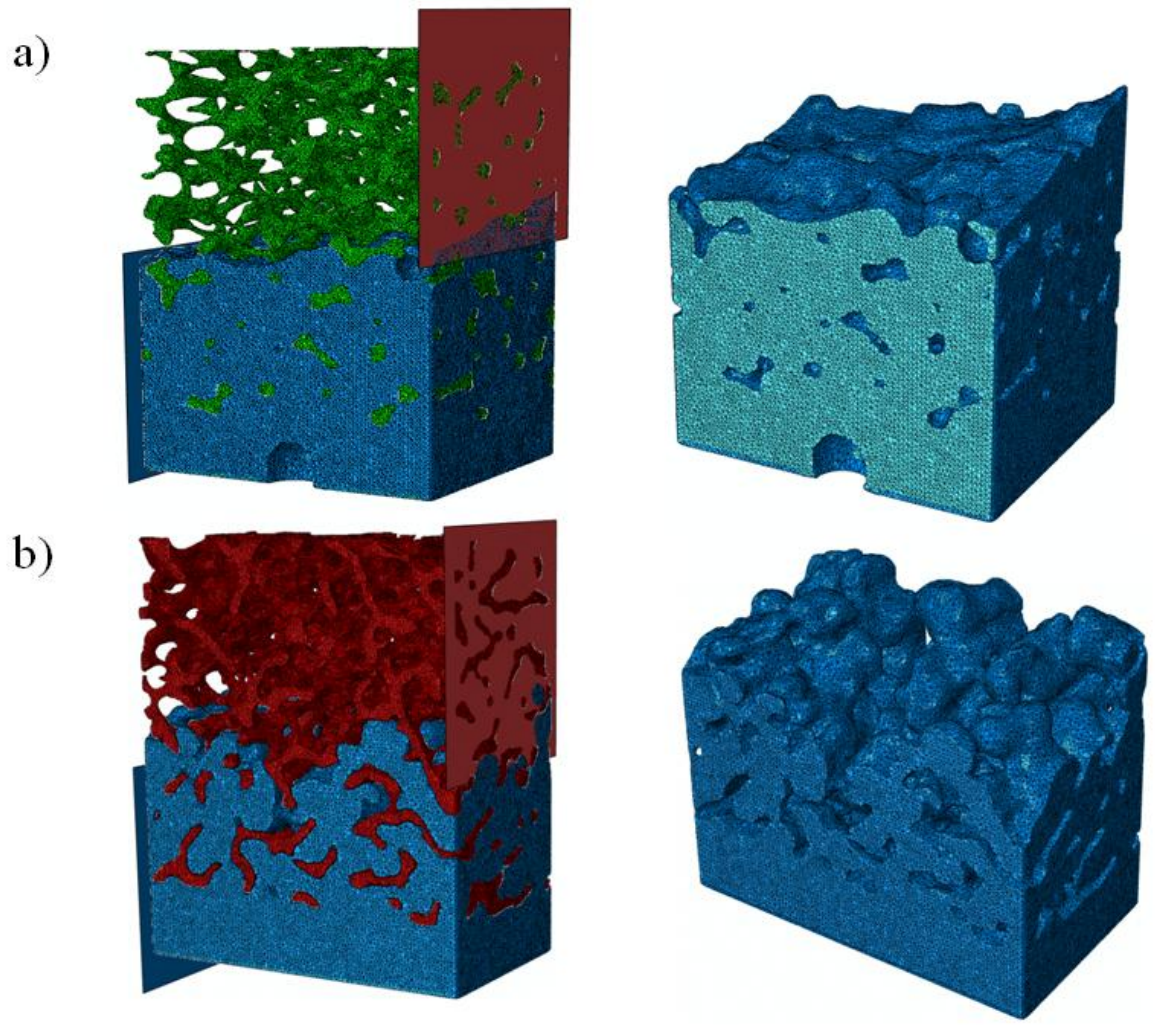

Fig.2 The finite element model of a (a) foam-cement and (b) bone-cement [21] composite samples generated from the μCT images of the specimen. The cement part of the models (blue) was isolated to show the two different morphologies of the interdigitated region. The two red planes indicate where the shear cut was applied at the interface on the two models (a-b).

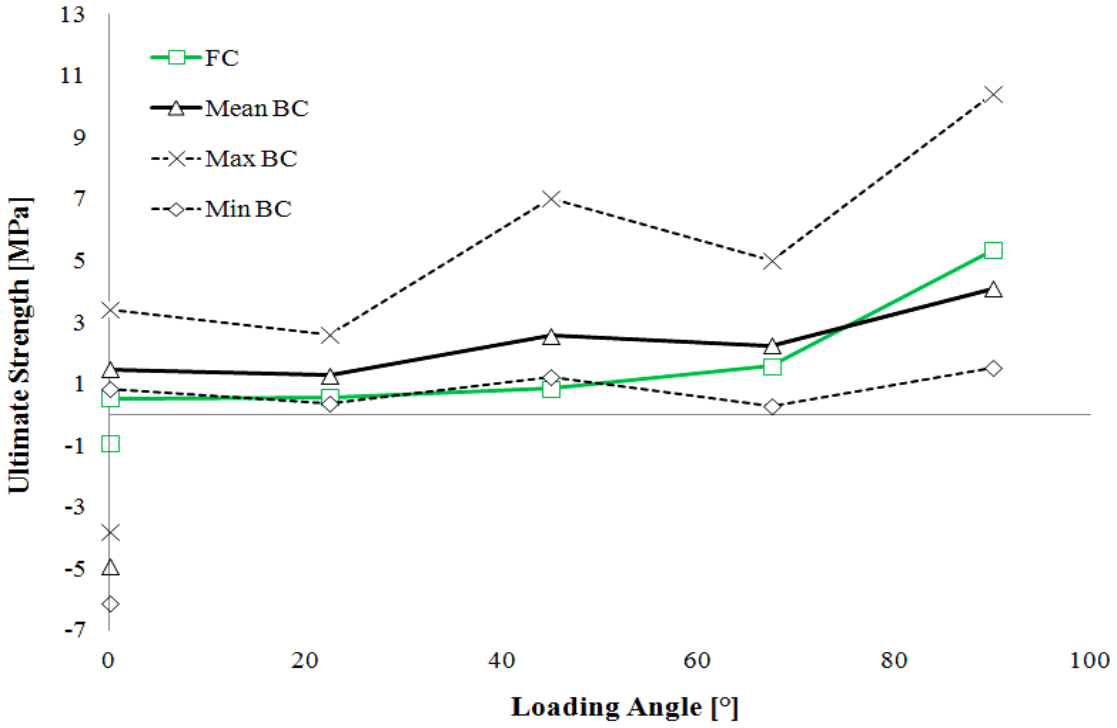

Fig.3 The apparent interfacial strength of the foam-cement interface (green) as a function of the loading angle. The results are compared with those obtained for bone-cement samples (black) tested under the same conditions and reported by Wang et al. [1] for tension, shear, mixed-mode and Tozzi et al. [2] for compression.

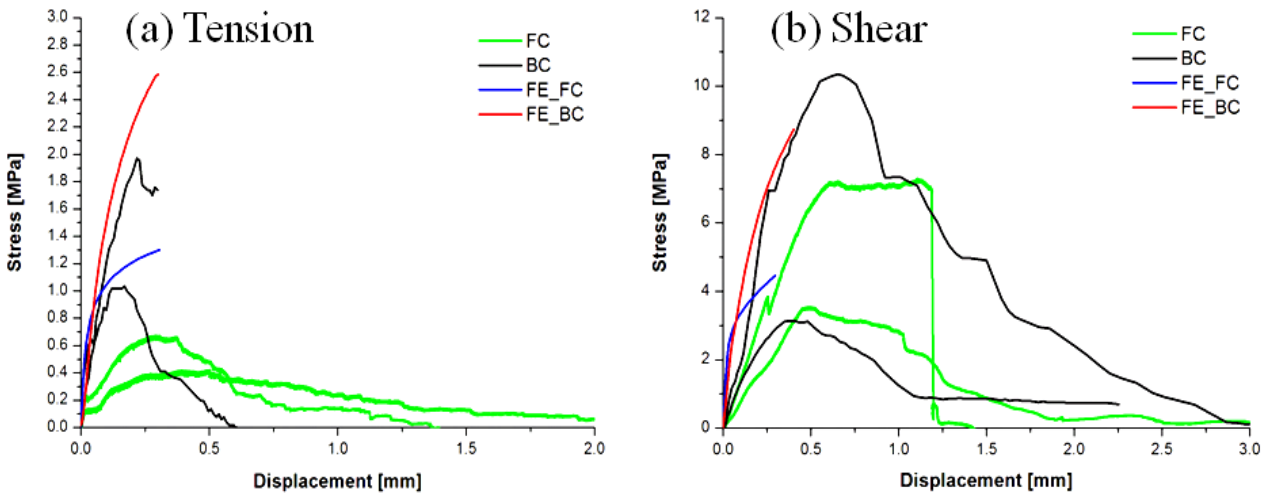

Fig.4 The experimental (green) and FE predicted (blue) stress-displacement curves of the foam-cement samples obtained under (a) tension and (b) shear loading conditions. Two typical experimental bone-cement responses [1] and the apparent stress-displacement predicted (red) by FE subject specific model [21] are used as comparison.

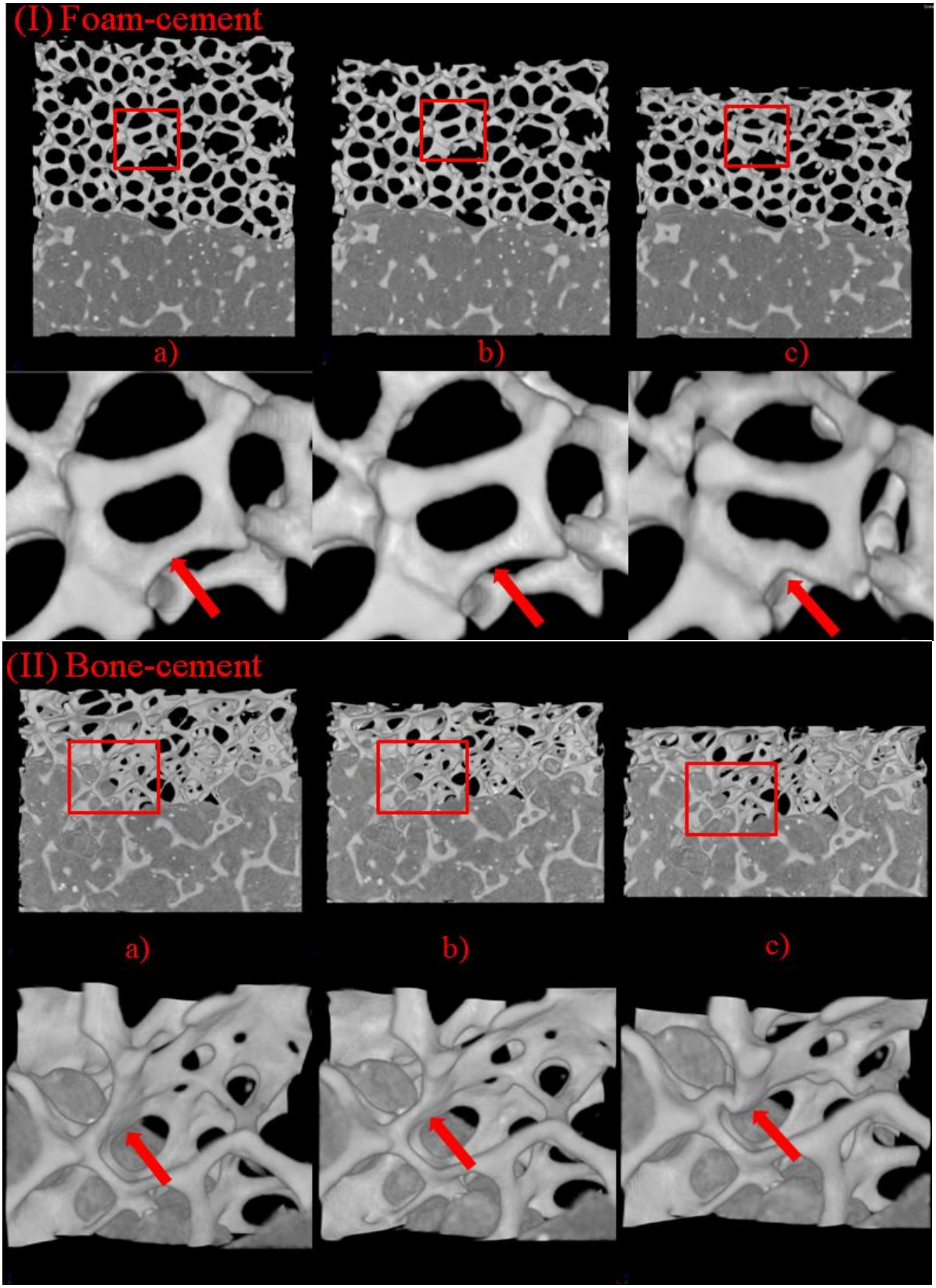

Fig.5 IGFA analysis of the foam-cement (I) and bone-cement (II) interface samples tested under step-wise compression and selected sub-volumes (rectangles), where the progressive microdamage was monitored: (a) unloaded; (b) at the ultimate stress; (c) failure state and (d) details of the local damage (mostly trabeculae and struts buckling), as indicated by the arrows. The bone-cement case (II) was adopted from Tozzi et al. [2].

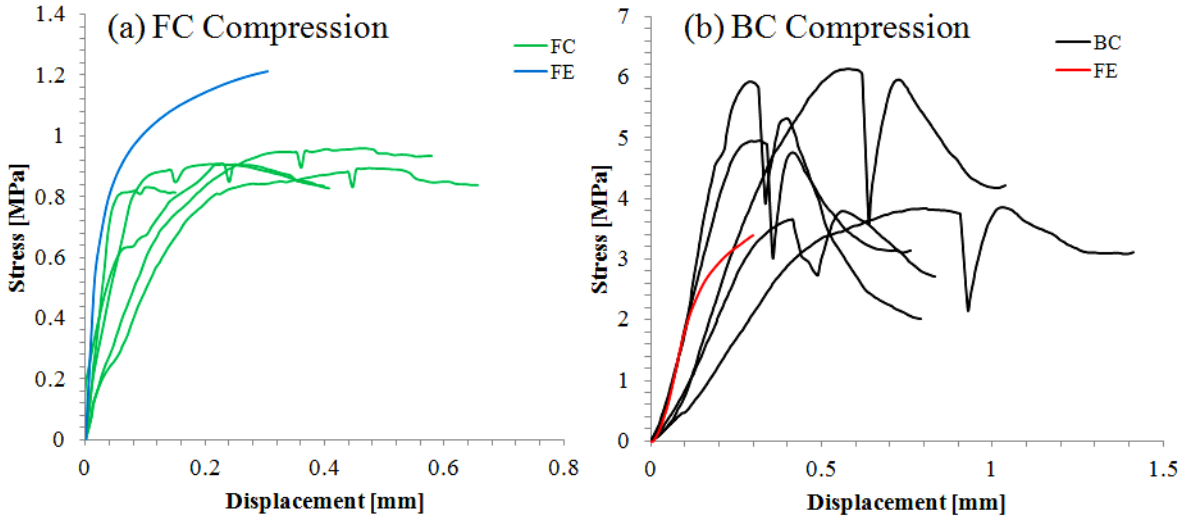

Fig.6 Comparison of the stress-displacement curves obtained from the compressive testing of (a) foam-cement and (b) bone-cement [2] samples, including the apparent stress-displacement relation predicted form the FE models.

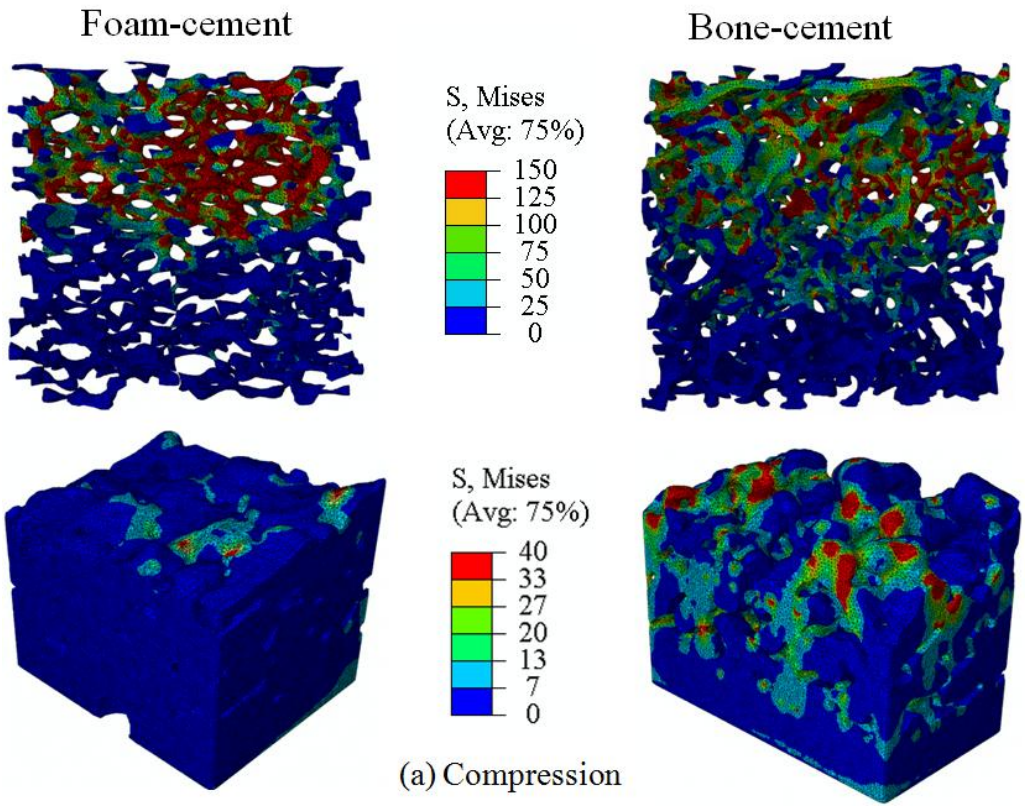

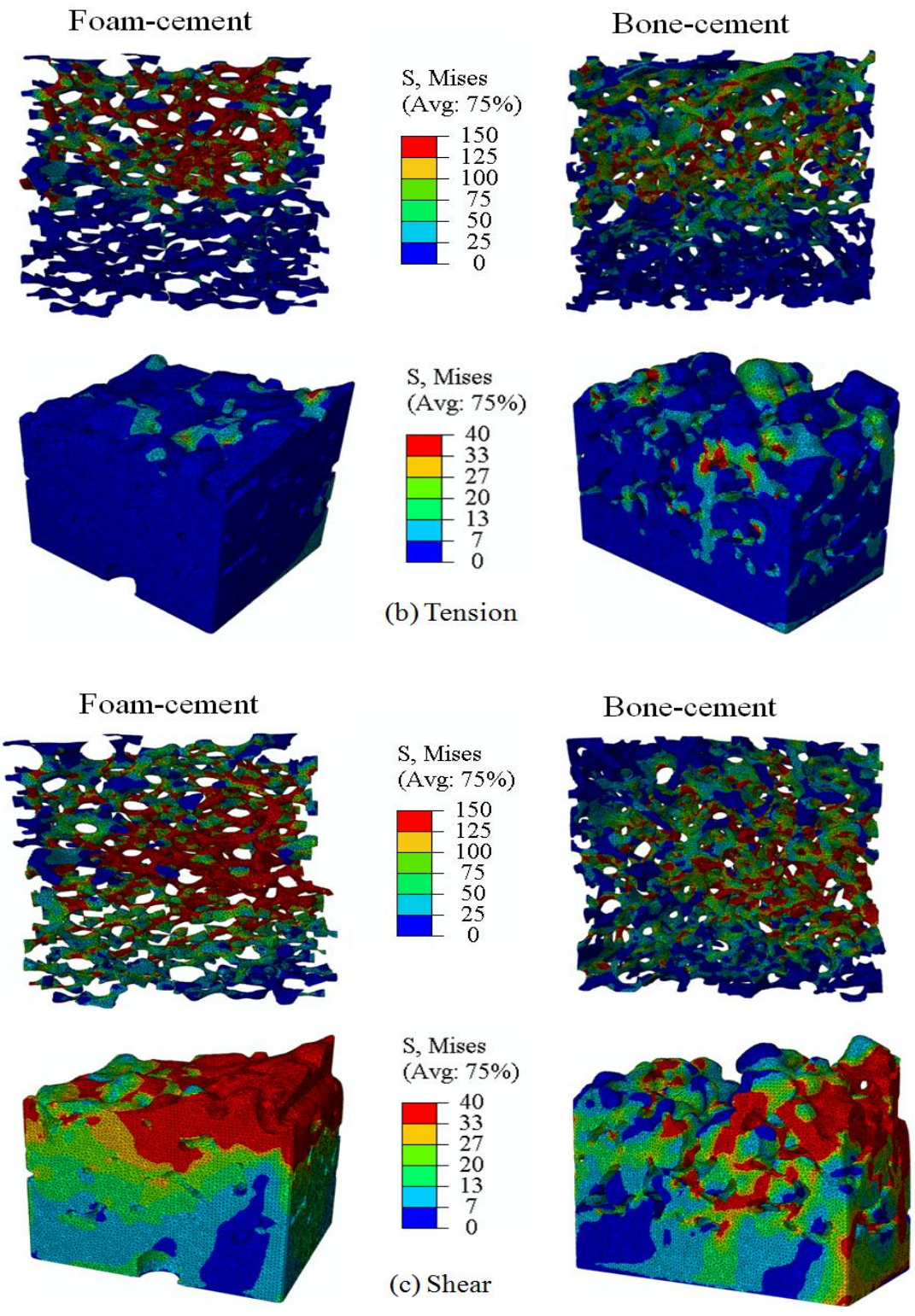

Fig.7 The local FE predicted stress distribution on the cellular and cement parts of the bone-cement and foam-cement samples under (a) compression, (b) tension and (c) shear loading conditions. The load transfer between bone/foam and cement appears to be more efficient in the bone-cement composite (cellular base material driven) under both compression and tension (a, b). Under shear (c) the loading condition seems to have obscured any difference in the cellular material properties.